Template Switching During Break-Induced Replication Is Promoted by the Mph1 Helicase in *Saccharomyces cerevisiae*

Anamarija Štafa,[1] Roberto A. Donnianni, Leonid A. Timashev, Alicia F. Lam, and Lorraine S. Symington[2]
Department of Microbiology and Immunology, Columbia University Medical Center, New York, New York 10032

ABSTRACT Chromosomal double-strand breaks (DSBs) that have only one end with homology to a donor duplex undergo repair by strand invasion followed by replication to the chromosome terminus (break-induced replication, BIR). Using a transformation-based assay system, it was previously shown that BIR could occur by several rounds of strand invasion, DNA synthesis, and dissociation. Here we describe a modification of the transformation-based assay to facilitate detection of switching between donor templates during BIR by genetic selection in diploid yeast. In addition to the expected recovery of template switch products, we found a high frequency of recombination between chromosome homologs during BIR, suggesting transfer of the DSB from the transforming linear DNA to the donor chromosome, initiating secondary recombination events. The frequency of BIR increased in the *mph1*Δ mutant, but the percentage of template switch events was significantly decreased, revealing an important role for Mph1 in promoting BIR-associated template switching. In addition, we show that the Mus81, Rad1, and Yen1 structure-selective nucleases act redundantly to facilitate BIR.

CHROMOSOMAL double-strand breaks (DSBs) are cytotoxic DNA lesions and if left unrepaired, or repaired incorrectly, can result in a loss of genetic information, genome instability, or even cell death. There are two main pathways to repair DSBs: homologous recombination (HR) and nonhomologous end joining (NHEJ). HR uses a homologous duplex to template repair of the break and is generally considered to be an error-free process; however, repair from a nonsister chromatid template can lead to loss of heterozygosity (LOH) or genome rearrangements (Symington 2002).

Initiation of HR requires degradation of the 5′-terminated strands to produce 3′-single-stranded DNA (ssDNA) tails that are first bound by replication protein A (RPA) and then replaced by Rad51 (Symington 2002). The Rad51 nucleoprotein filament searches for homologous sequences and promotes strand invasion to form a displacement loop (D-loop) (Figure 1). The 3′ end of the invading strand is used to prime DNA synthesis, templated by the donor duplex. The D-loop intermediate can be further channeled into one of several subpathways: synthesis-dependent strand annealing (SDSA), canonical double-strand break repair (DSBR), or break-induced replication (BIR). During SDSA, the invading strand that has been extended by DNA synthesis is displaced and anneals to complementary sequences exposed by 5′–3′ resection of the other side of the break. The remaining gaps can be filled by DNA synthesis and the nicks ligated to yield exclusively noncrossover products (Nassif *et al.* 1994; Ferguson and Holloman 1996). If the second end of the break is captured by the D-loop, a double Holliday junction (dHJ) can be generated after DNA repair synthesis and ligation (Szostak *et al.* 1983). dHJs can either be dissolved by the Sgs1–Top3–Rmi1 complex to form noncrossover products (Ira *et al.* 2003; Wu and Hickson 2003) or resolved by structure-selective nucleases to generate crossovers or noncrossovers. Mus81–Mms4 is the main nuclease responsible for mitotic crossovers in *Saccharomyces cerevisiae* with Yen1 serving as a back-up function (Blanco *et al.* 2010; Ho *et al.* 2010; Agmon *et al.* 2011; Muñoz-Galván *et al.* 2012). Mus81–Mms4

doi: 10.1534/genetics.114.162297
Manuscript received December 11, 2013; accepted for publication January 28, 2014; published Early Online February 4, 2014.
Available freely online through the author-supported open access option.
Supporting information is available online at http://www.genetics.org/lookup/suppl/doi:10.1534/genetics.114.162297/-/DC1.
[1]Present address: Laboratory for Biology and Microbial Genetics, Faculty of Food Technology and Biotechnology, University of Zagreb, Pierottijeva 6, 10000 Zagreb, Croatia.
[2]Corresponding author: College of Physicians and Surgeons, Columbia University Medical Center, 701 W. 168th St., New York, NY 10032. E-mail: lss5@columbia.edu

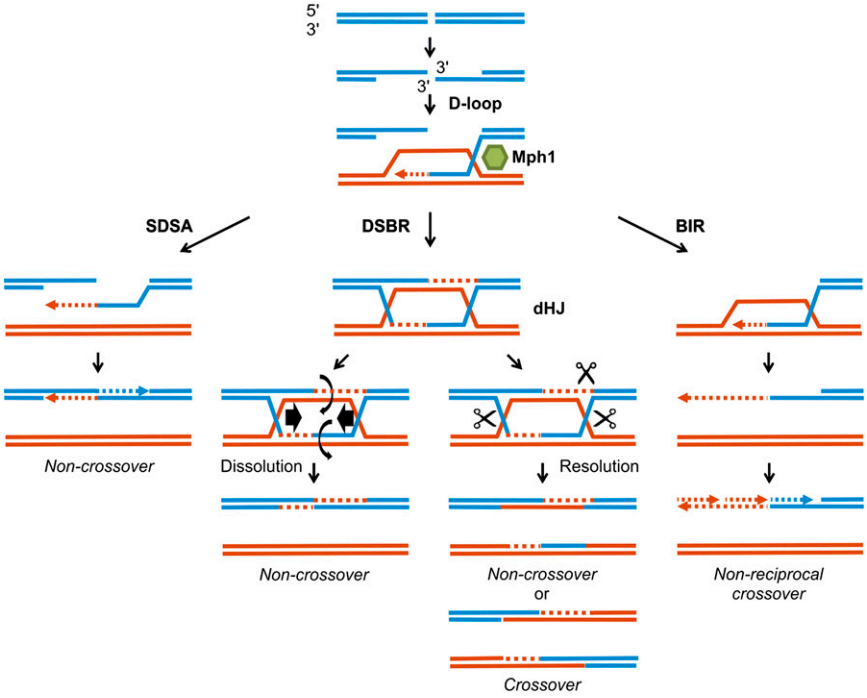

Figure 1 Models for homology-directed DSB repair. DNA end resection produces 3′ ssDNA tails that are utilized by Rad51 for the homology search and strand invasion to form a D-loop intermediate. After extension of the 3′ end in the context of the D-loop, the invading strand is thought to be displaced by a DNA helicase, such as Mph1, and to anneal to sequences on the other side of the DSB (SDSA). If the displaced strand of the D-loop pairs with the other side of the DSB, a double Holliday junction (dHJ) intermediate is formed after gap filling and ligation (DSBR). The dHJ intermediate can be dissolved by the Sgs1–Top3–Rmi1 complex or resolved by structure-selective nucleases. If homology is restricted to one DSB end, DNA synthesis can occur in the context of the D-loop to the chromosome terminus, referred to as BIR.

is also proposed to act on the captured D-loop intermediate, prior to maturation to a dHJ, to form exclusively crossover products (Osman *et al.* 2003; Mazón and Symington 2013).

BIR is a one-ended double-strand break repair mechanism in which DNA synthesis primed within the D-loop proceeds to the chromosome end, copying tens of kilobases (Morrow *et al.* 1997; Malkova *et al.* 2005). BIR is far more mutagenic than normal S-phase DNA synthesis and recent studies have shown the nascent strands are synthesized by a conservative mechanism, similar to other gene conversion reactions (Arcangioli 2000; Ira *et al.* 2006; Deem *et al.* 2011; Donnianni and Symington 2013; Saini *et al.* 2013). BIR is the mechanism proposed for alternative lengthening of telomeres in the absence of telomerase and plays a minor role in repair of internal chromosome DSBs that have two ends with homology to a donor duplex (McEachern and Haber 2006; Ho *et al.* 2010). However, it is a preferential pathway to generate LOH in old yeast cells (McMurray and Gottschling 2003), and microhomology-mediated BIR (MMBIR) has been implicated in genomic rearrangements (Hastings *et al.* 2009).

BIR is most easily studied by creating a DSB where just one of the two ends can undergo homology-dependent strand invasion (Bosco and Haber 1998; Davis and Symington 2004; Malkova *et al.* 2005; Lydeard *et al.* 2007). In previous work from this laboratory, we described a plasmid-based assay to detect BIR in yeast. The chromosome fragmentation vector (CFV) contains the *URA3* selectable marker, *SUP11*, *CEN4*, a tract of $(G_{1\text{-}3}T)_n$ to provide a site for telomere addition and a unique DNA segment to target invasion of chromosomal sequence (Morrow *et al.* 1997; Davis and Symington 2004). The CFV is linearized between the chromosome homology and telomere seeding sequence *in vitro* and used to transform yeast, selecting for Ura^+ colonies. Most transformants arise by *de novo* telomere addition to heal one end of the CFV and strand invasion at the other end into the endogenous yeast locus to copy the entire chromosome arm, yielding a stable chromosome fragment (CF). When performed in diploid cells with polymorphic copies of chromosome III, ~15% of the CFs recovered contained sequences from both chromosome homologs, suggesting the replication intermediate formed during BIR is unstable and the invading end can switch to a different template—a process referred to here as "template switching" (Smith *et al.* 2007). Template switching was observed not only between chromosome homologs but also between ectopic homologies on different chromosomes, revealing the potential for this mechanism to generate genome rearrangements. Template switching has also been reported during BIR initiated at a chromosomal DSB, indicating that it is a general phenomenon and not restricted to the plasmid system (Ruiz *et al.* 2009; Pardo and Aguilera 2012).

Template switching could be facilitated by helicases that displace the invading 3′ strand, as proposed for SDSA, or by cleavage of the D-loop intermediate by structure-selective nucleases (Pardo and Aguilera 2012). The obvious candidate for displacement of the 3′ strand during template switching is the Mph1 3′–5′ helicase, an ortholog of FANCM that displaces D-loops and extended D-loops following Rad51-mediated strand invasion (Sun *et al.* 2008; Prakash *et al.* 2009; Sebesta *et al.* 2011). Interestingly, when *MPH1* is overexpressed in yeast, it inhibits BIR at a chromosomal DSB but not at telomeres (Luke-Glaser and Luke 2012). The Pif1 5′–3′ helicase is required for mitochondrial DNA maintenance and functions in nuclear genome stability by unwinding

G quadruplexes and preventing *de novo* telomere addition at DSBs (Schulz and Zakian 1994; Ribeyre *et al.* 2009; Bochman *et al.* 2010; Paeschke *et al.* 2013). Recent studies identified a role for Pif1 during BIR (Hu *et al.* 2013; Saini *et al.* 2013; Wilson *et al.* 2013).

Here we describe a modification of the transformation assay to facilitate analysis of template switching associated with BIR in yeast. The assay is based on transformation of diploid yeast strains heteroallelic for *ade2* or *leu2* with CFVs that invade just upstream of the *ade2* or *leu2* locus. In addition to the expected recovery of CFs with a functional copy of *ADE2* or *LEU2* by template switching, recombination between the chromosome homologs targeted by the CFV occurred at a high frequency during BIR. The percentage of Ade^+ transformants was significantly decreased in the *mph1*Δ and *pif1-m2* mutants, and most of the Ade^+ events recovered from the *mph1*Δ mutant were due to chromosomal recombination, revealing an important role for Mph1 in template switching associated with BIR.

Materials and Methods

Media, growth conditions, and genetic methods

Rich medium (1% yeast extract, 2% peptone, 2% dextrose) (YPD), synthetic complete medium (SC) lacking the appropriate amino acids or nucleic acid bases, sporulation medium, and genetic methods were as described previously (Sherman *et al.* 1986). Rich medium supplemented with 2% galactose instead of dextrose was used for induction of *HO* endonuclease. Standard procedures were used for genetic crosses and transformation (Ito *et al.* 1983; Sherman *et al.* 1986).

Yeast strains and plasmids

S. cerevisiae strains used in this study are *RAD5* derivatives of W303 (Table 1). Strains containing ade2-I, ade2-n, his3Δ::hphMX4, his3Δ::natMX4, leu2ΔB, *leu2ΔR, mph1Δ::kanMX6, mus81Δ::kanMX6, rad1::LEU2, yen1Δ::HIS3, and pif1-m2* alleles were described previously (Mortensen *et al.* 2002; Wagner *et al.* 2006; Ho *et al.* 2010). All deletion alleles are denoted by Δ in the text. The *MET22* locus on the left arm of chromosome XV (Chr XV) was replaced by *TRP1* in the *ade2-n* strains. Diploids were made by crossing appropriate haploids to generate strains that were *MET22/met22::TRP1 ade2-I/ade2-n his3Δ::hphMX4/his3Δ::natMX4* or *leu2ΔR/leu2ΔB*.

CFVs used in this study are *ARS*$^-$ derivatives of CFV/D8B-tg (Davis and Symington 2004; Marrero and Symington 2010). Vectors pLAG6 and pLAG10 contain inserts from the right arm of Chr XV (Saccharomyces Genome Database, SGD coordinates 558476–563456 and 551748–556242, respectively) while vectors pLS192 and pLAG8 contain sequences from the left arm of Chr III (SGD coordinates 96821–102096 and 93450–98535, respectively).

Transformation-based template switching assays

ade2 assay: A total of 500 ng of *Bgl*II-digested pLAG6 or pLAG10 was used to transform competent yeast cells, selecting for Ura^+ transformants. The percentage of Ura^+ Ade^+ (white) was determined from the total number of Ura^+ transformants. All Ura^+ Ade^+ transformants were further analyzed by patching onto YPD medium to allow growth in nonselective conditions and then replica plating to 5-fluoroorotic acid (5-FOA)-containing medium to select for cells that became Ura^- due to loss of the CF (Boeke *et al.* 1984). Cells that lost the CF were scored again for their color, allowing distinction between 5-FOA red (Ade^-; W/R; template switching) and 5-FOA white (Ade^+; W/W; BIR-associated chromosomal recombination) transformants, and scored on SC −Met, SC −Trp, YPD +nourseothricin (Nat), and YPD +hygromycin B (Hyg) for marker loss. Ura^+ Ade^- transformants derived from pLAG6 in wild type, *mph1*Δ, and *mus81*Δ strains were also scored for the heterozygous markers on the left and right arms of Chr XV after CF loss. Pulsed-field gel electrophoresis of intact chromosomal DNA prepared from Ura^+ transformants was used to confirm formation of full-length CF products (Schwartz and Cantor 1984; Davis and Symington 2004).

leu2 assay: A total of 500 ng of linearized CFVs pLS192 and pLAG8, digested with *Sna*BI and *Bgl*II, respectively, was used to transform competent yeast cells, selecting for Ura^+ transformants. Transformants were replica plated on SC −Leu medium to determine the percentage that were Leu^+. Ura^+ Leu^+ transformants were further analyzed by patching on YPD, to allow growth in nonselective conditions and replica plated on 5-FOA to select for Ura^- cells that lost the CF, followed by replica plating to SC −Leu to distinguish between Leu^- (template switching) and Leu^+ (BIR-associated chromosomal recombination) transformants.

Statistical significance was determined after totaling Ade^+ and Leu^+ transformants from several independent transformations using two-tailed Pearson's chi-squared test (χ^2; http://in-silico.net/). For the *ade2* assay, the numbers of Ade^+ Ura^+ transformants were compared to Ade^- Ura^+ transformants (Figure 2D, Figure 4A, Figure 6A, and Supporting Information, Figure S3), while for the *leu2* assay Leu^+ Ura^+ transformants were compared to the number of Leu^- Ura^+ transformants (Figure 2D). To determine statistical significance of template switching *vs.* chromosomal recombination, the number of template switching transformants (W/R on 5-FOA) was compared to the number of BIR-associated chromosomal recombinants (W/W on 5-FOA; Figure 3A, Figure 4B, Figure 6B, and Figure S3). To determine the statistical significance of LOH for a specific transforming DNA and strain after growth of transformants on 5-FOA-containing medium, the number of transformants that lost Hyg or Nat resistance (LOH transformants) was compared to those with no LOH (Figure 3C and Figure S1).

BIR efficiency was determined using 500 ng of the specified linearized CVF or 100 ng of circular replicative plasmid pRS416 for each transformation, selecting for Ura^+ transformants. BIR efficiency is expressed as the ratio of Ura^+ transformants obtained per nanogram of CFV and per nanogram of

Table 1 Yeast strains

Strain	Genotype	Source
LSY2165-11C	*MATα ade2-I his3Δ::hphMX4 mus81Δ::kanMX6*	Ho *et al.* (2010)
LSY2165-30B	*MAT***a** *ade2-I his3Δ::hphMX4 mus81Δ::kanMX6 yen1Δ::HIS3*	Ho *et al.* (2010)
LSY2240	*MAT***a** *leu2::ΔEcoRI lys2*	Mortensen *et al.* (2002)
LSY2241	*MATα leu2::ΔBstell trp1-1*	Mortensen *et al.* (2002)
LSY2332-2B	*MATα ade2-I his3Δ::hphMX4 mph1Δ::kanMX6*	Mazón and Symington (2013)
LSY2543	*MAT***a** *met22::KlTRP1 ade2-n his3Δ::natMX4*	This study
LSY2633	*MAT***a** *met22::KlTRP1 ade2-n his3Δ::natMX4 mus81Δ::kanMX6*	This study
LSY2638	*MATα ade2-I his3Δ::hphMX4*	This study
LSY2650	*MATα ade2-I his3Δ::hphMX4 mph1Δ::kanMX6*	This study
LSY2653	*MAT***a** *met22::KlTRP1 ade2-n his3Δ::natMX4 mph1Δ::kanMX6*	This study
LSY2708-1D	*MAT***a** *ade2-I his3Δ::hphMX4 pif1-m2*	This study
LSY2709-4C	*MATα met22::KlTRP1 ade2-n his3Δ::natMX4 pif1-m2*	This study
LSY2738-15B, 16D	*MATα ade2-I his3Δ::hphMX4 mlh1Δ::kanMX6*	This study
LSY2739-8B	*MATα ade2-I his3Δ::hphMX4 mph1Δ::kanMX6 pif1-m2*	This study
LSY2739-16A	*MAT***a** *ade2-I his3Δ::hphMX4 mph1Δ::kanMX6 pif1-m2*	This study
LSY2740-8B, 19B	*MATα met22::KlTRP1 ade2-n his3Δ::natMX4 mus81Δ::kanMX6 yen1Δ::HIS3*	This study
LSY2802-5B	*MAT***a** *met22::KlTRP1 ade2-n his3Δ::natMX4 mph1Δ::kanMX6*	This study
LSY2803-7C	*MAT***a** *met22::KlTRP1 ade2-n his3Δ::natMX4 mlh1Δ::LEU2*	This study
LSY2804-5D	*MATα met22::KlTRP1 ade2-n his3Δ::natMX4 mph1Δ::kanMX6 pif1-m2*	This study
LSY2804-17A	*MAT***a** *met22::KlTRP1 ade2-n his3Δ::natMX4 mph1Δ::kanMX6 pif1-m2*	This study
LSY2950	*MAT***a**/*MATα leu2::ΔEcoRI/leu2::ΔBstell lys2/LYS2 trp1-1/TRP1*	This study
LSY2951	*MAT***a**/*MATα ade2-I/ade2-n his3Δ::hphMX4/his3Δ::natMX4 MET22/ met22::KlTRP1*	This study
LSY2332-2B × LSY2802-5B, LSY2650 × LSY2653	Identical to strain LSY2951 except *mph1Δ::kanMX6/mph1Δ::kanMX6*	This study
LSY2708-1D × LSY2709-4C	Identical to strain LSY2951 except *pif1-m2/pif1-m2*	This study
LSY2739-8B × LSY2804-17A, LSY2739-16A × LSY2804-5D	Identical to strain LSY2951 except *mph1Δ::kanMX6/mph1Δ::kanMX6 pif1-m2/pif1-m2*	This study
LSY2165-11C × LSY2633	Identical to strain LSY2951 except *mus81Δ::kanMX6/mus81Δ::kanMX6*	This study
LSY2165-30B × LSY2740-8B, LSY2165-30B × LSY2740-19B	Identical to strain LSY2951 except *mus81Δ::kanMX6/mus81Δ::kanMX6 yen1Δ::HIS3/ yen1Δ::HIS3*	This study
LSY2738-15B × LSY2803-7C, LSY2738-16D × LSY2803-7C	Identical to strain LSY2951 except *mlh1Δ::LEU2/mlh1Δ::LEU2*	This study
LSY2767-72D	*MAT***a**-*inc lys2::natMX4 AVT2::lysΔ3′-HOcs::kanMX6 SYN8::TRP1-5′Δys2 (Chr. I 128 kb) ade3::P_{GAL}-HO bar1::LEU2*	Donnianni and Symington (2013)
LSY2884-53D	Identical to strain LSY2767-72D except *mph1Δ::kanMX6*	This study
LSY2884-188C	Identical to strain LSY2767-72D except *pif1-m2*	This study
LSY2885-297B	Identical to strain LSY2767-72D except *URA3::GPD-TK7*	This study
LSY2885-160B, 248A	Identical to strain LSY2767-72D except *URA3::GPD-TK7 mus81Δ::kanMX6*	This study
LSY2885-121B, 127C	Identical to strain LSY2767-72D except *URA3::GPD-TK7 yen1Δ::HIS3*	This study
LSY2885-294A	Identical to strain LSY2767-72D except *mus81Δ::kanMX6 yen1Δ::HIS3*	This study
LSY2885-236A	Identical to strain LSY2767-72D except *mus81Δ::kanMX6 rad1::LEU2*	This study
LSY2886-1C, 51B	Identical to strain LSY2767-72D except *URA3::GPD-TK7 rad1::LEU2*	This study
LSY2921-10B, 42B	Identical to strain LSY2767-72D except *mus81Δ::kanMX6 rad1::LEU2 yen1Δ::HIS3*	This study
LSY2921-93D	Identical to strain LSY2767-72D except *rad1::LEU2 yen1Δ::HIS3*	This study

All strains are derived from the W303 background (*ade2-1 can1-100 his3-11, 15 leu2-3, 112 trp1-1 ura3-1*); only mating type and differences from this genotype are shown.

pRS416. The experiments were repeated at least three times for each CFV and strain. Mean BIR efficiencies were compared using Welch two-sample *t*-test from R Statistical software.

Chromosomal assay for BIR

Two-milliliter YPD cultures were grown overnight at 30°. Cells were diluted and regrown to OD_{600} 0.3–0.8 in YP with 2% raffinose and adjusted to an OD_{600} of 0.3. Aliquots of serial dilutions were plated on YPD, and SC −Lys and, for galactose induction, on YPGal plates and grown for 2–3 days. Colonies that grew on YPGal plates were replica plated to SC −Lys plates to ensure reconstitution of the functional *LYS2* gene by BIR. The percent BIR rate was calculated as the ratio of colony-forming units (CFUs) on SC −Lys after *HO* induction and CFUs on YPD (Donnianni and Symington 2013). Significance was determined using the Student's *t*-test.

Results

A genetic assay to detect template switching during BIR

We developed a simple genetic assay to screen candidate genes for their roles in template switching during BIR. Diploid yeast strains heteroallelic for *ade2* or *leu2* mutations

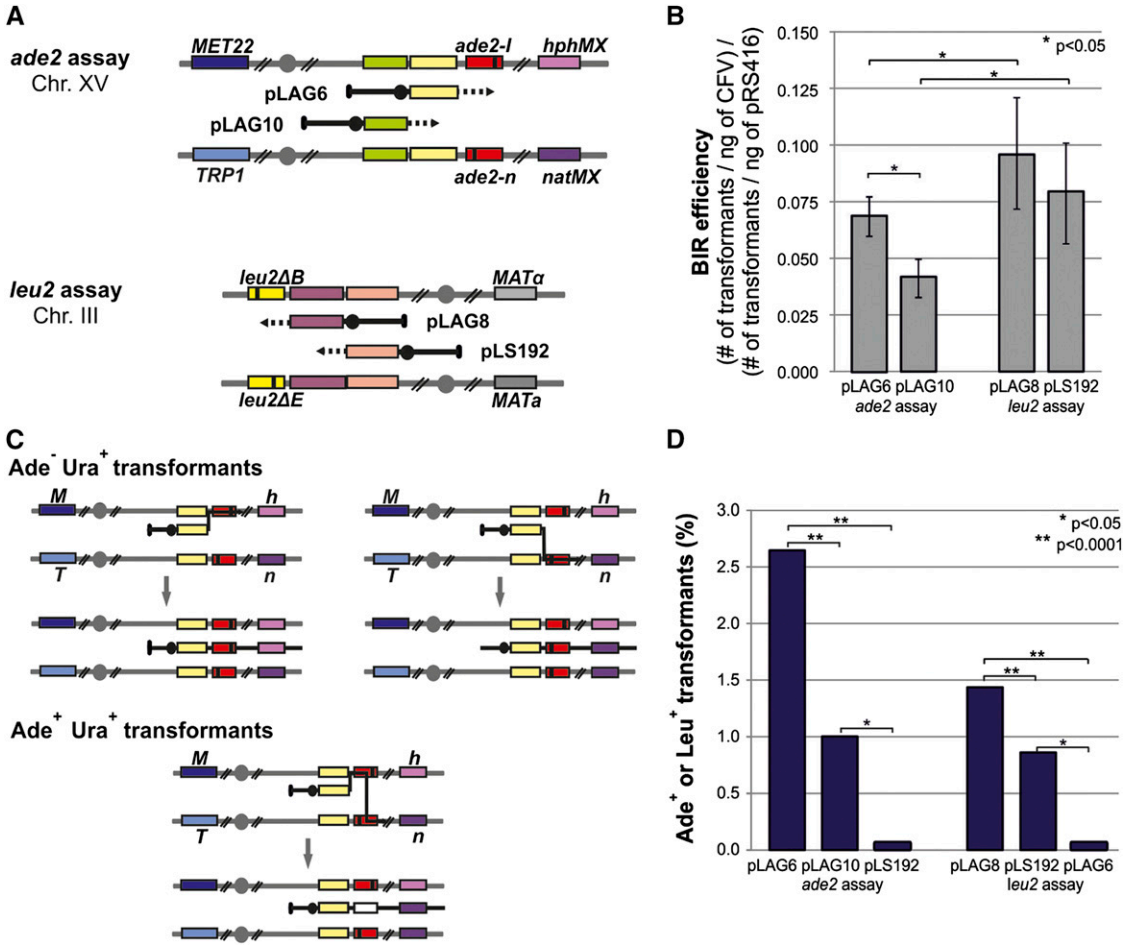

Figure 2 Template-switching assays. (A) Schematic showing the invasion sites for pLAG6 and pLAG10 on Chr XV and pLAG8 and pLS192 on Chr III. (B) BIR efficiencies for the indicated vectors in wild type. Transformations were performed five to nine times and mean values are presented with standard deviation (SD). (C) The simplest explanation for generation of Ura$^+$ Ade$^-$ transformants is by invasion of one of the two Chr XV homologs by the CFV, and the generation of Ura$^+$ Ade$^+$ transformants could result from invasion of *ade2-I*, displacement, and invasion of the *ade2-n* allele. (D) Percentage of Ade$^+$ or Leu$^+$ transformants in wild type for both assays. pLS192 serves as control in the *ade2* assay (invasion of a non-*ade2*-containing chromosome), and pLAG6 is a control in the *leu2* assay (invasion of a non-*leu2*-containing chromosome).

were transformed using linearized CFVs that invade upstream of the *ade2* or *leu2* loci and the resulting transformants were tested for adenine or leucine prototrophy, respectively. The strains for the *ade2* assay contain *ade2-I* and *ade2-n* alleles on Chr XV homologs (Mozlin *et al.* 2008); the mutations are 0.95 kb apart and both inactivate *ADE2*, resulting in accumulation of a red pigment. CFVs pLAG6 and pLAG10 contain sequences homologous to Chr XV to promote strand invasion 1 kb and 8 kb upstream of the *ade2* locus, respectively (Figure 2A). To confirm the generality of results from the *ade2* assay, *leu2* heteroalleles were used. The *leu2ΔB* and *leu2ΔE* mutations are 0.6 kb apart and inactivate *LEU2* on Chr III (Mortensen *et al.* 2002). CFVs pLAG8 and pLS192, which invade 1 and 4 kb upstream of the *leu2* region, respectively, were used for transformation (Figure 2A).

We first analyzed the BIR efficiency for both assays in cells with normal recombination functions ("wild type"); pLAG8 and pLAG192 have 30% higher BIR efficiency than pLAG6 and pLAG10 ($P = 0.013$ and $P = 0.008$, respectively). This difference could be explained by the shorter region of DNA that needs to be copied in the *leu2* assay as compared to the *ade2* assay (100 kb *vs.* 560 kb, respectively; Figure 2B) (Donnianni and Symington 2013).

Transformation of an *ade2-I/ade2-n* heteroallelic diploid with pLAG6 or pLAG10 results in generation of mainly red (Ade$^-$) Ura$^+$ transformants. The simplest mechanism to generate white Ade$^+$ Ura$^+$ transformants would be by invasion of Chr XV containing the *ade2-I* allele by the CFV and copying the 3′ part of the *ade2* gene followed by displacement of the invading strand and invasion of the *ade2-n* allele copying the 5′ part of the gene, resulting in formation of a functional *ADE2* gene carried on the CF (Figure 2C), though other mechanisms are possible. pLAG6, which invades closer to the *ade2* locus than pLAG10, resulted in 2.6-fold higher frequency of Ade$^+$ Ura$^+$ transformants compared to pLAG10 ($P < 0.0001$), in accordance with the previously observed 10-kb window from the invasion site in

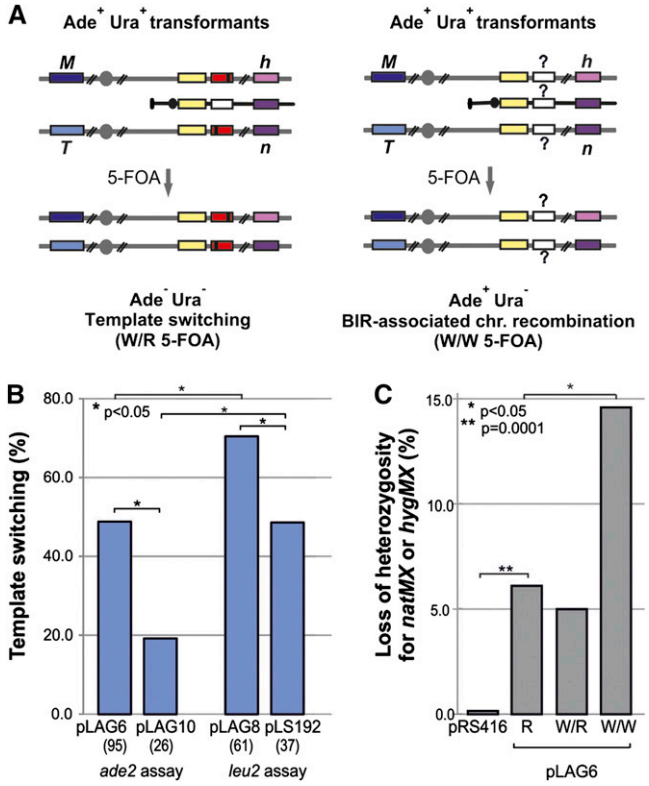

Figure 3 Chromosomal recombination associated with BIR. (A) Analysis of Ade+ transformants on 5-FOA plates to distinguish between template switching and BIR-associated chromosomal recombination. (B) Percent template switching for both assays in the wild type. Total number of Ade+ Ura+ and Leu+ Ura+ events analyzed for each vector is shown in parentheses. (C) LOH for the *natMX4* and *hphMX4* markers for wild type transformed with pLAG6 or pRS416. For pLAG6, Ura+ transformants were analyzed following loss of the CF by plating on 5-FOA-containing medium. R, Ade− transformants; W/R, Ade+ transformants that revert to Ade− after CF loss; and W/W, Ade+ transformants that remain Ade+ after CF loss.

which template switching occurs (Smith *et al.* 2007). In the *leu2* assay, pLAG8 yielded 1.8-fold more Ura+ Leu+ transformants than pLS192 ($P < 0.0001$). The frequency of Ade+ Ura+ transformants using pLAG6 was 22-fold higher as compared to pLS192 ($P < 0.0001$) while the frequency of Leu+ Ura+ transformants with pLAG8 was 28-fold higher than with pLAG6 ($P < 0.0001$), confirming that Ade+ Ura+ or Leu+ Ura+ transformants are a consequence of BIR upstream of the test locus and not caused by a genome-wide increase in spontaneous mitotic recombination during BIR (Figure 2D). Similarly, Ade+ Ura+ or Leu+ Ura+ transformants were only rarely recovered from transformation with the replicating plasmid pRS416. We acknowledge that only a small fraction of invasion, displacement, and reinvasion events are likely to generate Ade+ or Leu+ prototrophs and many template switch events will be genetically invisible.

BIR-induced chromosomal recombination

The Ade+ or Leu+ events due to template switching should have the *ADE2* or *LEU2* locus on the CF and after loss of the CF the cells would be expected to revert to an Ade− or Leu− phenotype. To test this prediction, Ade+ Ura+ or Leu+ Ura+ transformants were grown under nonselective conditions, replica plated to medium containing 5-FOA to select for Ura− cells that had lost the CF, and then analyzed for adenine or leucine prototrophy (Figure 3A). Surprisingly, only 47% or 19% of Ade+ transformants with pLAG6 or pLAG10, respectively, contained a CF-linked *ADE2* gene indicative of template switching. For the *leu2* assay, 70% and 49% of Leu+ transformants with pLAG8 and pLS192, respectively, were Leu− after CF loss (Figure 3B). Thus, a significant fraction of Ade+ and Leu+ transformants are due to BIR-induced recombination between chromosome homologs.

Induction of recombination between homologs was previously reported during plasmid gap repair and suggested to result from mismatch repair of a heteroduplex DNA intermediate (Silberman and Kupiec 1994). However, another possibility is that the D-loop intermediate is cleaved by a structure-selective nuclease effectively transferring the DSB from the linear fragment to the donor chromosome, initiating recombination with the homolog. The *ade2-I/ade2-n* diploids have additional heterozygous markers on Chr XV to evaluate chromosome loss or LOH for markers on the left or right arm (Ho *et al.* 2010). The *natMX4* and *hphMX4* markers are inserted 150 kb centromere proximal to the *ade2* locus. We expected heterozygosity for the flanking markers to be retained during BIR. However, if BIR-induced a chromosomal DSB, which initiated recombination between homologs, we would expect a significant fraction of the Ade+ chromosomal recombinants to exhibit LOH for the *natMX4* and *hphMX4* markers (Nickoloff *et al.* 1999; Barbera and Petes 2006; Ho *et al.* 2010). Seven of 48 (14.6%) white 5-FOA resistant colonies (W/W) derived from pLAG6 exhibited LOH for Nat or Hyg resistance (Figure 3C). Only 2 of 40 red 5-FOA resistant colonies (W/R) exhibited LOH for *natMX4* or *hphMX4*, but due to the low sample size this is not significantly less than observed for the chromosomal Ade+ events (W/W). Because the number of Ade+ transformants was low, we also analyzed Ura+ Ade− transformants to determine whether there was a general increase in LOH involving Chr XV homologs during BIR, regardless of whether template switching or chromosomal recombination occurred within the *ade2* locus. More than 500 Ade− Ura+ transformants derived from pLAG6 (R) were passaged on 5-FOA to lose the CF and then tested for LOH of the Chr XV markers. Of these, 31 (6.1%) exhibited LOH for Nat or Hyg resistance, one colony was Trp− Nat^s, indicative of chromosome loss, and one colony was Met−. The frequency of *natMX4* or *hphMX4* marker loss was significantly higher for the Ade+ colonies due to chromosomal recombination than for Ade− BIR events (R) ($P = 0.036$). Ura+ colonies obtained from transformation with pRS416 were also analyzed for marker loss and only 2/1185 tested showed LOH. The significant increase in LOH for the *natMX4* or *hphMX4* markers following transformation with pLAG6 compared with pRS416 ($P < 0.0001$) is consistent with induction of recombination between homologs during BIR.

Mph1 contributes to template switching during BIR

During SDSA, the extended invading 3′ end is displaced by helicases and, as proposed previously, displacement of the invading strand could facilitate template switching during BIR (Smith *et al.* 2007; Llorente *et al.* 2008). Therefore, we expected the inactivation of helicases that dissociate D-loop intermediates to increase the frequency of BIR, but to decrease the frequency of Ade$^+$ Ura$^+$ transformants. Mph1 has emerged as the main helicase responsible for SDSA in yeast since it is able to unwind Rad51 generated D-loops and DNA polymerase extended D-loops *in vitro*, and the *mph1*Δ mutant displays increased crossovers during mitotic recombination (Sun *et al.* 2008; Prakash *et al.* 2009; Tay *et al.* 2010; Sebesta *et al.* 2011; Mazón and Symington 2013; Mitchel *et al.* 2013). The percentage of Ade$^+$ Ura$^+$ transformants derived from pLAG6 was reduced by 3.9-fold in the *mph1*Δ mutant as compared to wild type (0.68%; $P < 0.0001$; Figure 4A). Furthermore, analysis of CF-cured Ade$^+$ Ura$^+$ transformants from the *mph1*Δ mutant revealed that only 23.8% were due to template switching, 2-fold less than wild type ($P = 0.0029$; Figure 4B). These results are in agreement with the role of Mph1 in the displacement of D-loops (Figure 5A). To determine whether maintenance of heterozygosity during BIR was affected by the *mph1*Δ mutation, 542 Ade$^-$ Ura$^+$ transformants derived from pLAG6 were grown on 5-FOA-containing medium to lose the CF and then tested for loss of Nat or Hyg resistance. The frequency of LOH for the *natMX4* and *hphMX4* markers was 7.4%, not significantly different from wild type (Figure S1).

Pif1 promotes BIR but does not affect template switching

We measured template switching in the *pif1-m2* mutant since previous studies have shown a decreased frequency of BIR in *pif1* mutants (Chung *et al.* 2010; Hu *et al.* 2013; Wilson *et al.* 2013). The *pif1-m2* allele expresses a form of Pif1 that retains mitochondrial activity, but is largely defective for nuclear function (Schulz and Zakian 1994). The percentage of Ade$^+$ Ura$^+$ transformants derived from pLAG6 was reduced by eightfold in the *pif1-m2* strain (0.31%; $P < 0.0001$), and even further decreased in the *mph1*Δ *pif1-m2* mutant (0.16%, $P = 0.031$ and $P < 0.001$ compared to *pif1-m2* and *mph1*Δ strains, respectively; Figure 4A), suggesting an additive effect of *MPH1* and *PIF1*. However, the proportion of Ade$^+$ events due to template switching was the same for *pif1-m2* and wild-type strains. The number of Ade$^+$ events recovered from the *mph1*Δ *pif1-m2* strain was very low and the percent due to template switching was not significantly different from the single mutants or wild type (Figure 4B).

Pif1 is a negative regulator of telomerase and the frequency of *de novo* telomere addition increases in the *pif1-m2* mutant (Schulz and Zakian 1994; Boule *et al.* 2005). To eliminate the possibility that Ura$^+$ transformants were generated by telomere addition at both ends of the linear vector,

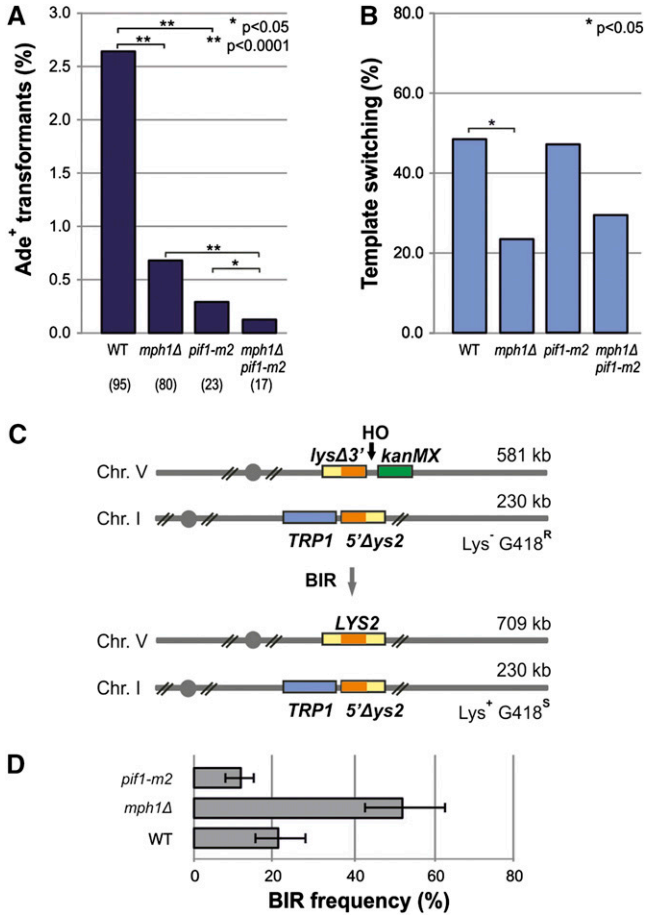

Figure 4 Mph1 promotes template switching during BIR. (A) Percentage of Ura$^+$ Ade$^+$ transformants and (B) template switching in the wild type (WT), *mph1*Δ, *pif1-m2*, and *mph1*Δ *pif1-m2* mutants transformed with linearized pLAG6. Total number of Ade$^+$ Ura$^+$ events analyzed for each strain is shown in parentheses. (C) Chromosomal BIR assay. A DSB 34 kb from the left telomere of Chr V is induced by plating on medium containing galactose. After DSB induction, the *kanMX6* gene and the chromosomal sequences distal to the break are lost, while Chr V invades the left arm of Chr I, and DNA synthesis restores a functional *LYS2* gene. The orange boxes indicate the extent of homology shared by the *lysΔ3′* and *5′Δys2* cassettes. (D) BIR frequency of the indicated mutants. Assays were performed five to six times and mean values with SD are presented.

independent Ura$^+$ transformants were analyzed by pulsed-field gel electrophoresis and all were confirmed to have full-length CF products (Figure S2). The heterozygous markers on the left and right arms of Chr XV can be used to monitor half-crossover events as an alternative product to BIR. Surprisingly, of 23 Ade$^+$ events analyzed from the *pif1-m2* mutant, only one was consistent with formation by a half crossover; thus, most of the CFs recovered result from BIR and not from half crossovers.

We could not accurately assess the BIR frequency of the *pif1-m2* mutant using the plasmid-based assay due to more efficient telomere healing at the telomere-seed sequence of the linear CFV leading to an artificially high transformation frequency (data not shown) (Schulz and Zakian 1994). To more accurately determine the BIR frequency of the *mph1*Δ

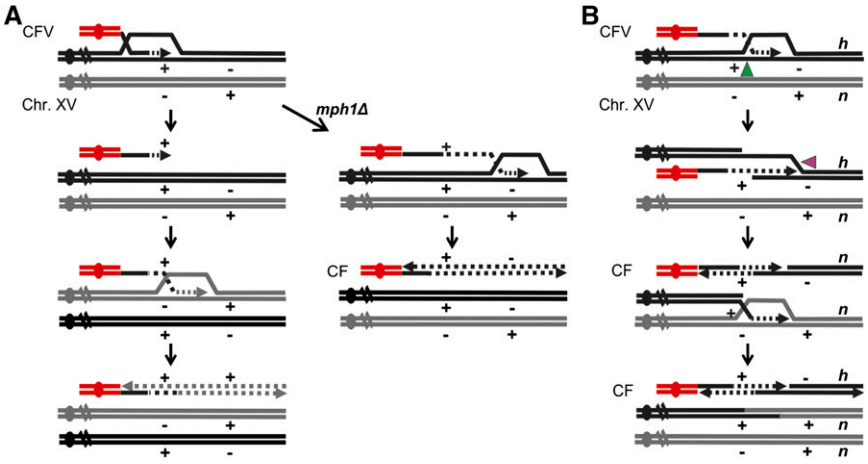

Figure 5 Models for template switching and chromosomal recombination associated with BIR. (A) The 3′ end of the CFV invades one homolog, and, after DNA synthesis to copy part of the *ade2* locus, is displaced by Mph1. In the absence of homologous sequences to pair with, the extended 3′ end invades the *ade2* locus of either homolog; if a different homolog is used, DNA synthesis can result in generation of a functional *ADE2* sequence. Continued replication to the chromosome terminus generates a CF. In the *mph1*Δ mutant, dissociation of the D-loop intermediate is decreased and replication from the initial strand invasion event proceeds to the telomere, resulting in fewer Ade$^+$ products. (B) If the initial strand invasion intermediate is cut by structure-selective nucleases, the CFV can become covalently linked to chromosomal sequences downstream of the site of strand invasion (half crossover). The resulting truncated chromosome can then invade the other homolog, generating a functional copy of *ADE2* and resulting in homozygosis of the downstream markers, or invade the newly formed CF (not shown) retaining heterozygosity for *natMX4* (*n*) and *hphMX4* (*h*) resistance.

and *pif1-m2* mutants, a chromosomal assay was used. The chromosomal assay is based on reconstitution of a functional *LYS2* gene by BIR (Donnianni and Symington 2013). A recipient cassette with a 3′-truncated *lys2* gene (designated *lys*Δ*3′*), a 36-bp HO endonuclease cut site (HO cs), and *kanMX6* to confer resistance to geneticin (G418) was inserted 34 kb from the left telomere of Chr V. There are no essential genes distal to the site of the insertion. A donor cassette composed of *TRP1* and a 5′ truncation of *lys2* (denoted by *5′*Δ*ys2*) was inserted 128 kb from the left telomere of Chr I (Figure 4C). The truncated *lys*Δ*3′* and *5′*Δ*ys2* genes share 2.1-kb homology. These donor and recipient cassettes were incorporated into a haploid strain with a deletion of the native *LYS2* locus, with the *MAT***a**-*inc* allele to prevent cleavage at the endogenous HO cs and which is capable of expressing *HO* from a galactose-regulated promoter. After DSB formation, the *lys*Δ*3′* sequence invades the donor cassette and copies to the end of Chr I, generating a Lys$^+$ nonreciprocal translocation product (Figure 4C). The other side of the Chr V DSB lacks homology to sequences in the yeast genome and is degraded, resulting in loss of the *kanMX6* gene and sensitivity to G418. The frequency of BIR was determined by the plating efficiency of cells on galactose-containing medium (*HO* constitutively expressed) that are Lys$^+$ G418^s relative to medium with glucose (*HO* off). The BIR frequency was reduced by 1.9-fold in the *pif1-m2* mutant ($P = 0.0076$), whereas the BIR frequency increased by 2.4-fold in the *mph1*Δ background ($P = 0.0002$) (Figure 4D). These results confirm previous studies showing positive and negative roles of *PIF1* and *MPH1*, respectively, during BIR (Luke-Glaser and Luke 2012; Hu *et al.* 2013; Saini *et al.* 2013; Wilson *et al.* 2013).

MUS81 is not required for BIR-associated template switching or chromosomal LOH

The increased LOH of the *natMX4* and *hphMX4* markers during BIR is consistent with transfer of the DSB from the CFV to the chromosome to initiate interhomolog recombination. Structure-selective nucleases could cleave the strand invasion intermediate resulting in several possible outcomes. Mus81–Mms4 cleavage of the D-loop, followed by gap filling and ligation, would be predicted to covalently link the CFV to the donor chromosome (Figure 5B). Subsequent cleavage of the front end of the D-loop would result in a half crossover, creating a CF and truncated donor chromosome. The broken chromosome could then engage in BIR with the chromosome homolog, resulting in LOH for *natMX4* or *hphMX4* and the potential to form an Ade$^+$ recombinant (Figure 5B). Alternatively, the truncated chromosome could invade the newly formed CF, retaining heterozygosity for *natMX4* and *hphMX4* after CF loss. The frequency of Ade$^+$ recombinants and the percent of Ade$^+$ events due to chromosomal recombination in the *mus81*Δ mutant were not significantly different from wild type (Figure 6). We also analyzed Ade$^-$ Ura$^+$ transformants from the *mus81*Δ mutant after growth on 5-FOA-containing medium to lose the CF; the frequency of LOH for Nat or Hyg resistance was 4.1%, not significantly different from wild type (Figure S1).

The failure to detect a decrease in chromosomal Ade$^+$ recombinants in the absence of Mus81 could be due to Yen1 cleavage of the BIR intermediate (Blanco *et al.* 2010; Ho *et al.* 2010; Agmon *et al.* 2011; Muñoz-Galván *et al.* 2012). Because the *mus81*Δ *yen1*Δ diploid grows very slowly and has low transformation efficiency we were unable to generate sufficient Ura$^+$ Ade$^+$ transformants for meaningful analysis. Furthermore, the spontaneous chromosome instability of the *mus81*Δ *yen1*Δ resulted in a high frequency of LOH (~2%) even in cells transformed with the replicative plasmid, pRS416, making it difficult to identify events associated with BIR (data not shown). Since the growth defect conferred by *mus81*Δ and *yen1*Δ is less in haploids than in diploids (Ho *et al.* 2010), we measured the BIR frequency of *mus81*Δ and *yen1*Δ mutants using the haploid chromosomal system. The *mus81*Δ and *yen1*Δ

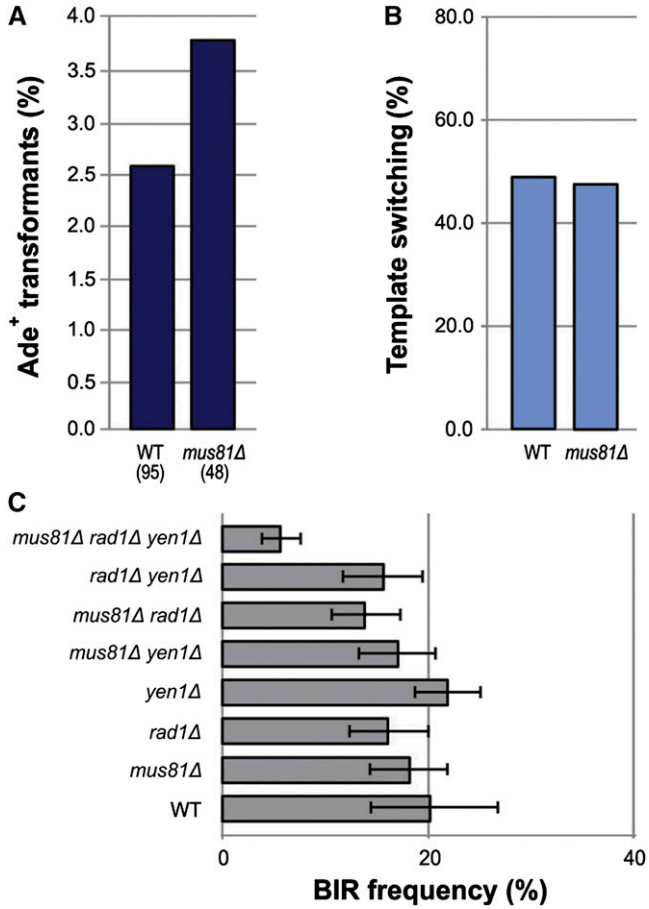

Figure 6 Role of structure-selective nucleases in BIR. Percentage of Ura$^+$ Ade$^+$ transformants (A) and template switching (B) in the *mus81*Δ mutant transformed with linearized pLAG6. Total number of Ade$^+$ Ura$^+$ events analyzed for each strain is shown in parentheses. (C) BIR frequencies of the indicated strains using the chromosomal assay. Assays were performed five to six times for each strain and mean values with SD are presented.

mutations did not affect the BIR frequency and no significant decrease was observed for the *mus81*Δ *yen1*Δ double mutant. We also tested the effect of deleting *RAD1* because the BIR assay involves recombination between limited homology substrates, and Rad1–Rad10 can be important to cleave intermediates with a branched structure adjacent to a heterology (Lyndaker and Alani 2009; Mazón *et al.* 2012). The BIR frequency was lower in the *mus81*Δ *rad1*Δ double mutant than in wild type ($P = 0.0003$) and reduced further in the *mus81*Δ *rad1*Δ *yen1*Δ triple mutant as compared to the *mus81*Δ *rad1*Δ mutant ($P = 0.0004$) (Figure 6C), indicating that the nucleases have overlapping roles in promoting BIR.

Mismatch repair does not influence template switching or Ade$^+$ chromosomal recombination

Ade$^+$ chromosomal recombinants could potentially occur through two rounds of mismatch repair of a heteroduplex DNA intermediate formed by pairing of an extended single strand from the CFV and one of the chromosome homologs (Ray *et al.* 1989; Silberman and Kupiec 1994). Therefore, we tested if eliminating the Mlh1 protein, an essential component of the mismatch repair system, which plays no role in processing branched DNA intermediates (Harfe and Jinks-Robertson 2000), would change either the percentage of Ade$^+$ transformants or the template switching/BIR-associated chromosomal recombination ratio. In both cases, data from the *mlh1*Δ mutant were the same as with wild type, with 1.78% Ade$^+$ transformants and 47.02% due to template switching (Figure S3), indicating that mismatch repair has no apparent role in template switching or chromosomal recombination during BIR.

Discussion

It has been previously shown that switching between DNA templates can occur during BIR and if it takes place between ectopic homologous sequences can result in genome rearrangements (Smith *et al.* 2007; Ruiz *et al.* 2009). The transformation-based assay using *ade2* heteroallelic diploids described here allows simplified detection of template switching events by a change of phenotype. Still, only those events that occur by switching between the *ade2-n* and *ade2-I* mutations (located 0.95 kb apart) are detected as Ade$^+$ recombinants and many template switch events are expected to be genetically invisible. In addition to template switching, we found a high frequency of events in which one of the chromosomal loci became Ade$^+$, reminiscent of earlier studies reporting "tripartite" recombination induced by a DSB on an ectopic template (Ray *et al.* 1989; Silberman and Kupiec 1994). Here, we investigated the roles of the helicases encoded by *MPH1* and *PIF1* in template switching associated with BIR.

The Mph1 helicase is known to catalyze dissociation of the invading strand of Rad51-generated D-loops or extended D-loops *in vitro* and consequently would be predicted to facilitate template switching during BIR (Sun *et al.* 2008; Prakash *et al.* 2009; Sebesta *et al.* 2011). In agreement with a previous study (Luke-Glaser and Luke 2012) we found the frequency of BIR to be increased in the *mph1*Δ mutant, which we interpret to be due to Mph1-catalyzed dissociation of the invading 3′ end and the need for additional strand invasion events to complete BIR. The percentage of Ura$^+$ transformants that were Ade$^+$ was reduced in the *mph1*Δ mutant and template switching among the Ade$^+$ events was also decreased, consistent with the need for Mph1 to dismantle the D-loop for template switching. In the *mph1*Δ mutant, the more stable D-loop intermediate might more readily transition to a migrating D-loop after recruitment of Pif1 (Wilson *et al.* 2013) or be cut by structure-selective nucleases leading to secondary recombination events. The Ade$^+$ transformants recovered from the *mph1*Δ mutant were mainly due to chromosomal recombination, consistent with the idea that the stabilized D-loop is cleaved by structure-selective nucleases. If the D-loop were cut by nucleases to create a half crossover, linking the CFV to

sequences downstream of the site of strand invasion, the fragmented chromosome would likely engage with the homolog to repair the one-ended DSB by BIR, resulting in homozygosis of the downstream marker. Indeed, we found that 6.1 and 7.4% of all Ura$^+$ transformants derived from pLAG6 in the wild-type and *mph1*Δ strains, respectively, exhibited LOH for the *natMX4* or *hphMX4* markers after loss of the CF, suggesting secondary BIR events between a fragmented Chr XV and its homolog.

The frequency of BIR using a Chr III disome assay is decreased in the *pif1*Δ mutant and the products recovered are mainly due to half crossovers, similar to the phenotype observed for the *pol32*Δ mutant (*POL32* encodes a nonessential subunit of DNA polymerase δ) (Deem *et al.* 2008; Smith *et al.* 2009; Chung *et al.* 2010; Saini *et al.* 2013; Wilson *et al.* 2013). Loss of Pif1 also prevents Rad51-dependent telomere elongation in the absence of telomerase (Hu *et al.* 2013). In a reconstituted *in vitro* assay, Pif1 was shown to function with the DNA polymerase δ complex to extend the 3′ end of a Rad51-generated D-loop (Wilson *et al.* 2013). Pif1 facilitated extensive DNA synthesis by liberating the newly synthesized ssDNA to establish a migrating D-loop. We could not accurately assess the BIR frequency in the *pif1-m2* mutant using the CFV system because the increased efficiency of telomere elongation from the minimal telomere seed sequence of the CFV counteracted the decrease in BIR (data not shown). A more accurate assessment of the BIR frequency was obtained using the chromosomal BIR assay, revealing a twofold decrease in the *pif1-m2* mutant. The *pif1-m2* mutant is reported to retain some nuclear function and this might account for the higher BIR frequency than reported using the *pif1*Δ mutant (Schulz and Zakian 1994; Hu *et al.* 2013; Wilson *et al.* 2013). The fraction of Ade$^+$ events among Ura$^+$ transformants was significantly reduced in the *pif1-m2* strain, but we did not observe a change in the ratio of template switching and chromosomal recombination associated with BIR, suggesting Pif1 plays no role in D-loop dissociation.

In agreement with a previous study (Silberman and Kupiec 1994), we observed a high frequency of recombination between chromosome homologs induced by the linear transforming DNA. Ray *et al.* (1989) also reported stimulation of triparental recombination by a chromosomal DSB. In the previous studies, chromosomal conversion was suggested to result from mismatch repair of an hDNA intermediate; however, we observed no effect on the frequency of this class of events in an *mlh1*Δ mutant. Instead, the high frequency of LOH for the *natMX4* and *hphMX4* markers is more consistent with transfer of the DSB from the CFV to the chromosome triggering secondary recombination events. A high frequency of LOH for Nat or Hyg resistance was observed for all Ura$^+$ transformants derived from pLAG6, regardless of whether they were Ade$^+$ or Ade$^-$, suggesting a significant number of BIR intermediates are cleaved by structure-selective nucleases. Mus81–Mms4 cleaves model D-loop structures *in vitro* and could create the first cleavage necessary to form a half crossover with another nuclease

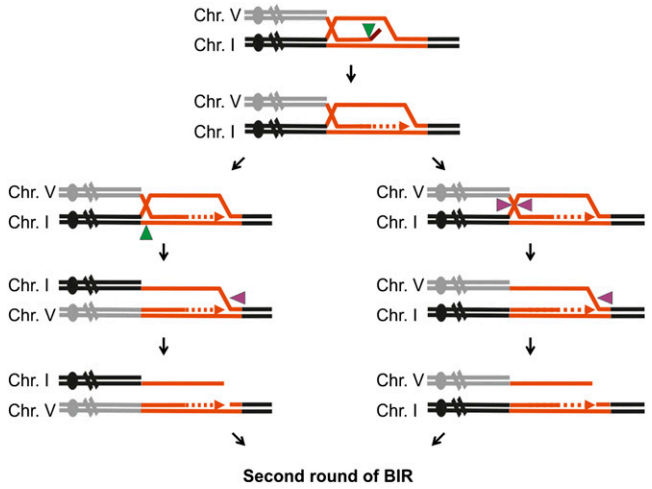

Figure 7 Model for how structure-selective nucleases promote BIR. After strand invasion, the heterology represented by the HO cs needs to be removed to allow extension of the 3′ end by DNA synthesis. Cleavage of the trailing end of the D-loop intermediate coupled with cleavage of the 5′ flap represented at the leading end of the D-loop would collapse the recombination intermediate, and the truncated chromosomes would need to engage in a second round of BIR to form viable products.

cutting the 5′ flap represented by the leading edge of the D-loop to complete the event (Osman *et al.* 2003). Slx1–Slx4 is able to cleave a variety of branched structures, including 5′ flaps, and Yen1/GEN1 also cuts 5′ flaps in addition to HJs (Fricke and Brill 2003; Rass *et al.* 2010). The frequency of LOH for total Ura$^+$ transformants (after selection for loss of the CF) from the *mus81*Δ mutant was not significantly less than observed for wild type, and chromosomal recombinants were recovered at a similar frequency to wild type. Thus, Mus81–Mms4 either does not play a major role in formation of half crossovers or Yen1, Rad1–Rad10, and Slx1–Slx4 act redundantly with it. Pardo and Aguilera (2012) reported a decreased frequency of half crossovers to circularize Chr III in the absence of Mus81, Yen1, and Slx1, suggesting these nucleases function redundantly to process branched DNA structures.

Recent studies show BIR occurs by a migrating D-loop mechanism resulting in conservative inheritance of the nascent strands (Donnianni and Symington 2013; Saini *et al.* 2013; Wilson *et al.* 2013). Structure-selective nucleases are not predicted to function in BIR by this mechanism, but could be required if progression of the D-loop stalls and requires restart by cleavage and reinvasion. Using the chromosomal assay, the frequency of BIR was unaffected in any of the nuclease single mutants, but we did find a significant decrease in the *mus81*Δ *rad1*Δ double mutant and a further decrease in the *mus81*Δ *rad1*Δ *yen1*Δ triple mutant, suggesting most of the BIR events detected in this system require cleavage of a branched DNA intermediate. The requirement for Rad1–Rad10 could be to remove the heterology presented by the HO cs sequence that would prevent pairing between the 3′ end and donor template or to cleave at the

heterology boundary if the D-loop intermediate branch migrated to the end of the homology shared by the *lys2* sequences (Figure 7) (Fishman-Lobell and Haber 1992). Mus81 is in the same family of nucleases as Rad1 and there is some evidence for overlapping functions to process recombination intermediates between limited homology substrates (Schwartz and Heyer 2011; Mazón *et al.* 2012). Yen1 could potentially cut the front end of the D-loop or the crossed strands resulting from strand invasion. The products of these cleavage events would necessitate a second cycle of BIR to form viable products.

In summary, our data support the hypothesis that Mph1 is the main helicase responsible for template switching during BIR. Unexpectedly, we observed a high frequency of LOH for Chr XV markers located 150 kb downstream of the site of strand invasion during BIR. We suggest these events are due to cleavage of the strand invasion intermediate, transferring the DSB from the linear CFV to the chromosome to initiate secondary BIR events, further increasing the genomic instability associated with this mutagenic DNA repair mechanism.

Acknowledgments

We thank L. Goss, H. Chen, and R. Rothstein for generous gifts of CFVs and yeast strains and members of the Symington lab for discussions and critical reading of the manuscript. This study was supported by a grant from the National Institutes of Health (R01 GM094386). R.A.D. is supported by an International Fellowship in Cancer Research cofunded by Associazione Italiana per la Ricerca sul Cancro and Marie Curie Actions.

Literature Cited

Agmon, N., M. Yovel, Y. Harari, B. Liefshitz, and M. Kupiec, 2011 The role of Holliday junction resolvases in the repair of spontaneous and induced DNA damage. Nucleic Acids Res. 39: 7009–7019.

Arcangioli, B., 2000 Fate of *mat1* DNA strands during mating-type switching in fission yeast. EMBO Rep. 1: 145–150.

Barbera, M. A., and T. D. Petes, 2006 Selection and analysis of spontaneous reciprocal mitotic cross-overs in *Saccharomyces cerevisiae*. Proc. Natl. Acad. Sci. USA 103: 12819–12824.

Blanco, M. G., J. Matos, U. Rass, S. C. Ip, and S. C. West, 2010 Functional overlap between the structure-specific nucleases Yen1 and Mus81-Mms4 for DNA-damage repair in *S. cerevisiae*. DNA Repair (Amst.) 9: 394–402.

Bochman, M. L., N. Sabouri, and V. A. Zakian, 2010 Unwinding the functions of the Pif1 family helicases. DNA Repair (Amst.) 9: 237–249.

Boeke, J. D., F. LaCroute, and G. R. Fink, 1984 A positive selection for mutants lacking orotidine-5′-phosphate decarboxylase activity in yeast: 5-fluoro-orotic acid resistance. Mol. Gen. Genet. 197: 345–346.

Bosco, G., and J. E. Haber, 1998 Chromosome break-induced DNA replication leads to nonreciprocal translocations and telomere capture. Genetics 150: 1037–1047.

Boule, J. B., L. R. Vega, and V. A. Zakian, 2005 The yeast Pif1p helicase removes telomerase from telomeric DNA. Nature 438: 57–61.

Chung, W. H., Z. Zhu, A. Papusha, A. Malkova, and G. Ira, 2010 Defective resection at DNA double-strand breaks leads to *de novo* telomere formation and enhances gene targeting. PLoS Genet. 6: e1000948.

Davis, A. P., and L. S. Symington, 2004 *RAD51*-dependent break-induced replication in yeast. Mol. Cell. Biol. 24: 2344–2351.

Deem, A., K. Barker, K. Vanhulle, B. Downing, A. Vayl *et al.*, 2008 Defective break-induced replication leads to half-crossovers in *Saccharomyces cerevisiae*. Genetics 179: 1845–1860.

Deem, A., A. Keszthelyi, T. Blackgrove, A. Vayl, B. Coffey *et al.*, 2011 Break-induced replication is highly inaccurate. PLoS Biol. 9: e1000594.

Donnianni, R. A., and L. S. Symington, 2013 Break-induced replication occurs by conservative DNA synthesis. Proc. Natl. Acad. Sci. USA 110: 13475–13480.

Ferguson, D. O., and W. K. Holloman, 1996 Recombinational repair of gaps in DNA is asymmetric in *Ustilago maydis* and can be explained by a migrating D-loop model. Proc. Natl. Acad. Sci. USA 93: 5419–5424.

Fishman-Lobell, J., and J. E. Haber, 1992 Removal of nonhomologous DNA ends in double-strand break recombination: the role of the yeast ultraviolet repair gene *RAD1*. Science 258: 480–484.

Fricke, W. M., and S. J. Brill, 2003 Slx1-Slx4 is a second structure-specific endonuclease functionally redundant with Sgs1-Top3. Genes Dev. 17: 1768–1778.

Harfe, B. D., and S. Jinks-Robertson, 2000 DNA mismatch repair and genetic instability. Annu. Rev. Genet. 34: 359–399.

Hastings, P. J., G. Ira, and J. R. Lupski, 2009 A microhomology-mediated break-induced replication model for the origin of human copy number variation. PLoS Genet. 5: e1000327.

Ho, C. K., G. Mazón, A. F. Lam, and L. S. Symington, 2010 Mus81 and Yen1 promote reciprocal exchange during mitotic recombination to maintain genome integrity in budding yeast. Mol. Cell 40: 988–1000.

Hu, Y., H. B. Tang, N. N. Liu, X. J. Tong, W. Dang *et al.*, 2013 Telomerase-null survivor screening identifies novel telomere recombination regulators. PLoS Genet. 9: e1003208.

Ira, G., A. Malkova, G. Liberi, M. Foiani, and J. E. Haber, 2003 Srs2 and Sgs1-Top3 suppress crossovers during double-strand break repair in yeast. Cell 115: 401–411.

Ira, G., D. Satory, and J. E. Haber, 2006 Conservative inheritance of newly synthesized DNA in double-strand break-induced gene conversion. Mol. Cell. Biol. 26: 9424–9429.

Ito, H., Y. Fukuda, K. Murata, and A. Kimura, 1983 Transformation of intact yeast cells treated with alkali cations. J. Bacteriol. 153: 163–168.

Llorente, B., C. E. Smith, and L. S. Symington, 2008 Break-induced replication: What is it and what is it for? Cell Cycle 7: 859–864.

Luke-Glaser, S., and B. Luke, 2012 The Mph1 helicase can promote telomere uncapping and premature senescence in budding yeast. PLoS ONE 7: e42028.

Lydeard, J. R., S. Jain, M. Yamaguchi, and J. E. Haber, 2007 Break-induced replication and telomerase-independent telomere maintenance require Pol32. Nature 448: 820–823.

Lyndaker, A. M., and E. Alani, 2009 A tale of tails: insights into the coordination of 3′ end processing during homologous recombination. Bioessays 31: 315–321.

Malkova, A., M. L. Naylor, M. Yamaguchi, G. Ira, and J. E. Haber, 2005 *RAD51*-dependent break-induced replication differs in kinetics and checkpoint responses from *RAD51*-mediated gene conversion. Mol. Cell. Biol. 25: 933–944.

Marrero, V. A., and L. S. Symington, 2010 Extensive DNA end processing by Exo1 and Sgs1 inhibits break-induced replication. PLoS Genet. 6: e1001007.

Mazón, G., and L. S. Symington, 2013 Mph1 and Mus81-Mms4 prevent aberrant processing of mitotic recombination intermediates. Mol. Cell 52: 63–74.

Mazón, G., A. F. Lam, C. K. Ho, M. Kupiec, and L. S. Symington, 2012 The Rad1-Rad10 nuclease promotes chromosome translocations between dispersed repeats. Nat. Struct. Mol. Biol. 19: 964–971.

McEachern, M. J., and J. E. Haber, 2006 Break-induced replication and recombinational telomere elongation in yeast. Annu. Rev. Biochem. 75: 111–135.

McMurray, M. A., and D. E. Gottschling, 2003 An age-induced switch to a hyper-recombinational state. Science 301: 1908–1911.

Mitchel, K., K. Lehner, and S. Jinks-Robertson, 2013 Heteroduplex DNA position defines the roles of the Sgs1, Srs2, and Mph1 helicases in promoting distinct recombination outcomes. PLoS Genet. 9: e1003340.

Morrow, D. M., C. Connelly, and P. Hieter, 1997 "Break copy" duplication: a model for chromosome fragment formation in *Saccharomyces cerevisiae*. Genetics 147: 371–382.

Mortensen, U. H., N. Erdeniz, Q. Feng, and R. Rothstein, 2002 A molecular genetic dissection of the evolutionarily conserved N terminus of yeast Rad52. Genetics 161: 549–562.

Mozlin, A. M., C. W. Fung, and L. S. Symington, 2008 Role of the *Saccharomyces cerevisiae* Rad51 paralogs in sister chromatid recombination. Genetics 178: 113–126.

Muñoz-Galván, S., C. Tous, M. G. Blanco, E. K. Schwartz, K. T. Ehmsen *et al.*, 2012 Distinct roles of Mus81, Yen1, Slx1-Slx4, and Rad1 nucleases in the repair of replication-born double-strand breaks by sister chromatid exchange. Mol. Cell. Biol. 32: 1592–1603.

Nassif, N., J. Penney, S. Pal, W. R. Engels, and G. B. Gloor, 1994 Efficient copying of nonhomologous sequences from ectopic sites via P-element-induced gap repair. Mol. Cell. Biol. 14: 1613–1625.

Nickoloff, J. A., D. B. Sweetser, J. A. Clikeman, G. J. Khalsa, and S. L. Wheeler, 1999 Multiple heterologies increase mitotic double-strand break-induced allelic gene conversion tract lengths in yeast. Genetics 153: 665–679.

Osman, F., J. Dixon, C. L. Doe, and M. C. Whitby, 2003 Generating crossovers by resolution of nicked Holliday junctions: a role for Mus81-Eme1 in meiosis. Mol. Cell 12: 761–774.

Paeschke, K., M. L. Bochman, P. D. Garcia, P. Cejka, K. L. Friedman *et al.*, 2013 Pif1 family helicases suppress genome instability at G-quadruplex motifs. Nature 497: 458–462.

Pardo, B., and A. Aguilera, 2012 Complex chromosomal rearrangements mediated by break-induced replication involve structure-selective endonucleases. PLoS Genet. 8: e1002979.

Prakash, R., D. Satory, E. Dray, A. Papusha, J. Scheller *et al.*, 2009 Yeast Mph1 helicase dissociates Rad51-made D-loops: implications for crossover control in mitotic recombination. Genes Dev. 23: 67–79.

Rass, U., S. A. Compton, J. Matos, M. R. Singleton, S. C. Ip *et al.*, 2010 Mechanism of Holliday junction resolution by the human GEN1 protein. Genes Dev. 24: 1559–1569.

Ray, A., N. Machin, and F. W. Stahl, 1989 A DNA double chain break stimulates triparental recombination in *Saccharomyces cerevisiae*. Proc. Natl. Acad. Sci. USA 86: 6225–6229.

Ribeyre, C., J. Lopes, J. B. Boule, A. Piazza, A. Guedin *et al.*, 2009 The yeast Pif1 helicase prevents genomic instability caused by G-quadruplex-forming CEB1 sequences *in vivo*. PLoS Genet. 5: e1000475.

Ruiz, J. F., B. Gomez-Gonzalez, and A. Aguilera, 2009 Chromosomal translocations caused by either pol32-dependent or pol32-independent triparental break-induced replication. Mol. Cell. Biol. 29: 5441–5454.

Saini, N., S. Ramakrishnan, R. Elango, S. Ayyar, Y. Zhang *et al.*, 2013 Migrating bubble during break-induced replication drives conservative DNA synthesis. Nature 502: 389–392.

Schulz, V. P., and V. A. Zakian, 1994 The Saccharomyces *PIF1* DNA helicase inhibits telomere elongation and de novo telomere formation. Cell 76: 145–155.

Schwartz, D. C., and C. R. Cantor, 1984 Separation of yeast chromosome-sized DNAs by pulsed field gradient gel electrophoresis. Cell 37: 67–75.

Schwartz, E. K., and W. D. Heyer, 2011 Processing of joint molecule intermediates by structure-selective endonucleases during homologous recombination in eukaryotes. Chromosoma 120: 109–127.

Sebesta, M., P. Burkovics, L. Haracska, and L. Krejci, 2011 Reconstitution of DNA repair synthesis *in vitro* and the role of polymerase and helicase activities. DNA Repair (Amst.) 10: 567–576.

Sherman, F., G. Fink, and J. Hicks, 1986 *Methods in Yeast Genetics*, Cold Spring Harbor Laboratory Press, Cold Spring Harbor, NY.

Silberman, R., and M. Kupiec, 1994 Plasmid-mediated induction of recombination in yeast. Genetics 137: 41–48.

Smith, C. E., B. Llorente, and L. S. Symington, 2007 Template switching during break-induced replication. Nature 447: 102–105.

Smith, C. E., A. F. Lam, and L. S. Symington, 2009 Aberrant double-strand break repair resulting in half crossovers in mutants defective for Rad51 or the DNA polymerase delta complex. Mol. Cell. Biol. 29: 1432–1441.

Sun, W., S. Nandi, F. Osman, J. S. Ahn, J. Jakovleska *et al.*, 2008 The FANCM ortholog Fml1 promotes recombination at stalled replication forks and limits crossing over during DNA double-strand break repair. Mol. Cell 32: 118–128.

Symington, L. S., 2002 Role of *RAD52* epistasis group genes in homologous recombination and double-strand break repair. Microbiol. Mol. Biol. Rev. 66: 630–670.

Szostak, J. W., T. L. Orr-Weaver, R. J. Rothstein, and F. W. Stahl, 1983 The double-strand-break repair model for recombination. Cell 33: 25–35.

Tay, Y. D., J. M. Sidebotham, and L. Wu, 2010 Mph1 requires mismatch repair-independent and -dependent functions of MutSalpha to regulate crossover formation during homologous recombination repair. Nucleic Acids Res. 38: 1889–1901.

Wagner, M., G. Price, and R. Rothstein, 2006 The absence of Top3 reveals an interaction between the Sgs1 and Pif1 DNA helicases in *Saccharomyces cerevisiae*. Genetics 174: 555–573.

Wilson, M. A., Y. Kwon, Y. Xu, W. H. Chung, P. Chi *et al.*, 2013 Pif1 helicase and Poldelta promote recombination-coupled DNA synthesis via bubble migration. Nature 502: 393–396.

Wu, L., and I. D. Hickson, 2003 The Bloom's syndrome helicase suppresses crossing over during homologous recombination. Nature 426: 870–874.

Communicating editor: N. Hollingsworth

GENETICS

Supporting Information
http://www.genetics.org/lookup/suppl/doi:10.1534/genetics.114.162297/-/DC1

Template Switching During Break-Induced Replication Is Promoted by the Mph1 Helicase in *Saccharomyces cerevisiae*

Anamarija Štafa, Roberto A. Donnianni, Leonid A. Timashev, Alicia F. Lam, and Lorraine S. Symington

DOI: 10.1534/genetics.114.162297

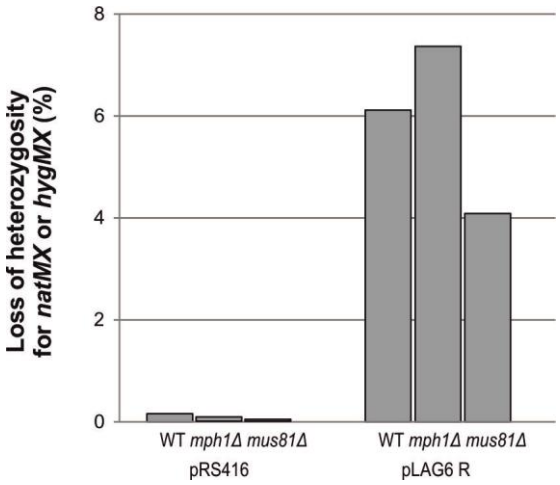

Figure S1 Loss of heterozygosity during BIR. Ura$^+$ transformants derived from pRS416 or pLAG6 were tested for LOH of the *natMX4* and *hphMX4* markers by direct replica plating (pRS416), or after selection for loss of the CF (pLAG6).

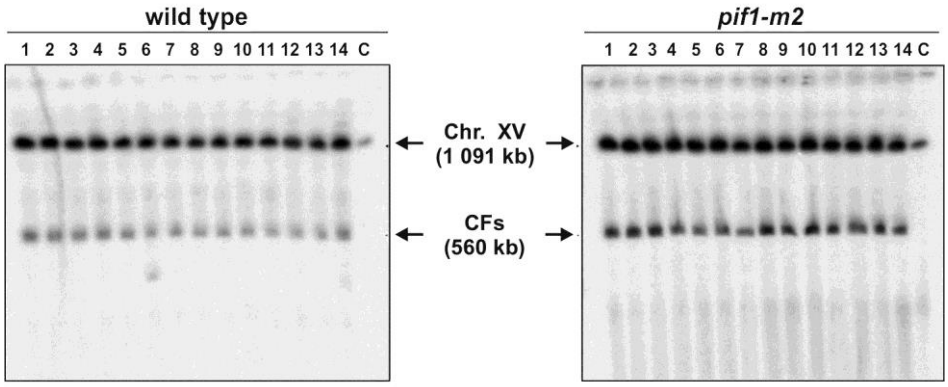

Figure S2 Pulsed field gel electrophoresis (PFGE) analysis of CF and Chr. XV size in wild type and *pif1-m2* mutant. Ura$^+$ transformants obtained from pLAG6 were analyzed by PFGE and Southern blot hybridization using an *ADE2* probe. Independent transformants from wild type (left panel) or *pif1-m2* (right panel) are shown; C refers to the untransformed strains.

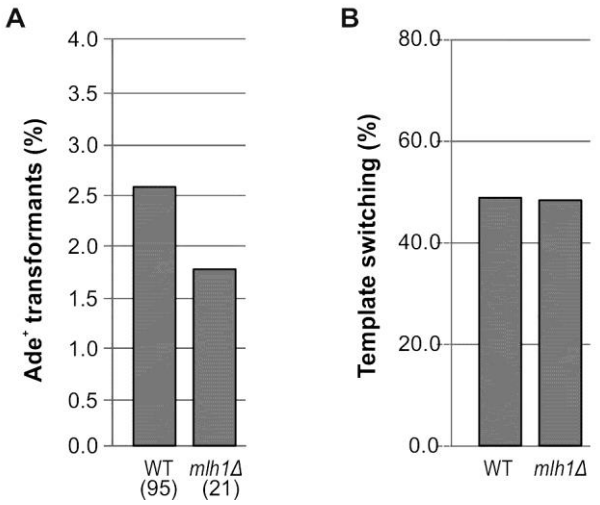

Figure S3 Mismatch repair is not required for chromosomal conversion. Percentage of Ura$^+$ Ade$^+$ transformants (A) and template switching (B) in the *mlh1Δ* mutant. Total number of Ade$^+$ Ura$^+$ events analyzed for each strain is shown in parenthesis.